Selenocentric Distant Retrograde Orbit Stability Assessments

1. Introduction

In association with NASA's asteroid strategy published 10 April 2013[*], selenocentric distant retrograde orbits (SDROs) have assumed a new importance in the field of astronautics. The strategy's asteroid redirect mission (ARM) concept advocates a small near-Earth asteroid (NEA) be brought to "a stable orbit in trans-lunar space" where astronauts would rendezvous with it. In its "Asteroid Redirect Mission Reference Concept" published 27 June 2013[†], NASA elaborates on ARM's final destination.

> The storage orbit for the redirected asteroid is a stable distant retrograde orbit (DRO) in the Earth-Moon system with an orbit altitude of ~70,000 km above the lunar surface.

This paper takes an empirical approach to assessing SDRO stability at initial conditions whose lunar distance is progressively increased. Initial conditions are coasted through time t using numeric integration [1] of point-mass gravitational accelerations from the Earth, Sun, and Moon. A conservative fixed integration time step of 600 s is adopted for all coasts. This is in accord with integration convergence findings from [1] applied to circular selenocentric orbits whose radii exceed 2160 km[‡]. To ensure these findings are not violated by excessive selenocentric speed at eccentricities approaching unity, any coast will be deemed unstable if it reaches a selenocentric distance less than 4300 km[§]. Over coasting intervals as long as 100 years, SDRO stability is equated with the degree to which selenocentric distance is confined. Therefore, a coast departing the Moon's vicinity is also deemed unstable[**].

Coast initial conditions are specified with respect to two selenocentric coordinate systems. Initial position and velocity can be expressed with Cartesian UVW components such that the unit vector $+\boldsymbol{U}$ points away from Earth, $+\boldsymbol{W}$ is the osculating unit vector of the Moon's geocentric angular momentum, and $\boldsymbol{V} = \boldsymbol{W} \times \boldsymbol{U}$ in the right-handed convention[††]. Initial position and velocity can also be expressed with Cartesian components in the Earth mean equator and equinox of epoch J2000.0 (J2K) coordinate system. Every coast is initiated at 30.5 June 2013 coordinate

---

[*] Reference "NASA's FY2014 Asteroid Strategy", available for download at http://www.nasa.gov/pdf/740684main_LightfootBudgetPresent0410.pdf (accessed 11 August 2013).

[†] This document is available for download at http://www.nasa.gov/pdf/756122main_Asteroid%20Redirect%20Mission%20Reference%20Concept%20Description.pdf (accessed 25 August 2013).

[‡] A selenocentric circular orbit of this radius would require 15 of the 600 s integration steps to span one orbit. The integrator is well converged under these conditions.

[§] At this distance, selenocentric escape speed is very nearly equal to speed in the selenocentric circular orbit of radius 2160 km, about 1.5 km/s.

[**] In this context, "vicinity" is not equivalent to the Moon's gravitational sphere of influence because 70,000 km is technically just outside that sphere. A working definition of vicinity would be twice this distance or ~140,000 km.

[††] Selenocentric velocity in UVW components is expressed by fixing each axis in inertial space at an associated epoch. In reality, these axes rotate in inertial space with the Earth-Moon line such that $\boldsymbol{U}$ always coincides with it.

time (CT)[‡‡], when the Moon's geocentric position $\boldsymbol{r}_M$ and velocity $\boldsymbol{v}_M$ have the following J2K components.

$$\boldsymbol{r}_M = \begin{bmatrix} +379{,}429.973 \\ +67{,}549.008 \\ +50{,}039.677 \end{bmatrix} \text{ km} \qquad \boldsymbol{v}_M = \begin{bmatrix} -0.145779 \\ +0.940908 \\ +0.329229 \end{bmatrix} \text{ km/s}$$

An SDRO's initial position is in the $+\boldsymbol{U}$ direction at a selenocentric distance r_0. Initial velocity is in the $-\boldsymbol{V}$ direction at a circular selenocentric speed $v_0 = \sqrt{\mu / r_0}$ assuming conic orbit motion with the Moon's reduced mass $\mu = 4902.798$ km^3/s^2 [2]. As r_0 is increased, the conic orbit motion assumption for v_0 tends to break down due to Earth and Sun gravity perturbations.

If a coast of conic v_0 departs the Moon's vicinity or approaches within 4300 km in less than 100 years, it can be differentially corrected according to circular restricted three-body problem (CRTBP) theory. A necessary condition for simple periodic symmetric orbits in CRTBP theory dictates the $\boldsymbol{V} = 0$ plane is crossed orthogonally exactly twice per orbit [3, Section 2.6.6.1]. Since a subset of periodic symmetric orbits contains SDROs, boundary conditions for v_0 differential correction are adopted as $+r_0\,\boldsymbol{U}$ at $t = 0$ and $\pm r_0\,\boldsymbol{U}$ at $t = t_1$. Iterations on t_1 are performed until selenocentric inertial flight path angles γ_0 at $t = 0$ and γ_1 at $t = t_1$ are small in magnitude, and each iteration achieves its specified $t = t_1$ position to within 0.1 km. Differentially corrected initial velocity v_0' is then coasted and assessed for stability.

Differential corrections to v_0 do not seek exactly zero γ_0 and γ_1 because associated coasts from $t = 0$ to $t = t_1$ are modeling accelerations consistent with uncorrected coasts initialized using v_0. All coasts, including those iterating to a differential correction, deviate from CRTBP theory because the Moon's geocentric orbit is not circular and solar gravity is simulated.

In some contexts, this paper will assess a selenocentric distant *prograde* orbit (SDPO) analogous to the SDRO primarily under study. These supplemental SDPO assessments are intended to convey the degree to which retrograde selenocentric orbit motion is critical to stability.

A useful metric in assessing an SDRO or SDPO for stability is the tally of ascending node crossings k on the Moon's true equator made during a coast. For example, suppose multiple 100-year coasts from similar initial conditions all stay in the Moon's vicinity without approaching within 4300 km. The coast with minimal k is typically the most stable because its mean eccentricity is also minimal among the 100-year coasts.

Before assessing SDROs for stability, the following section introduces a distant retrograde orbit occurring naturally in our solar system. This example illustrates the stability to be expected from SDROs and establishes a scaling reference for r_0.

[‡‡] A uniform time scale void of leap seconds, CT is used as the fundamental ephemeris argument by the Jet Propulsion Laboratory's (JPL's) online ephemeris system *Horizons* [2]. To a precision of ±0.002 s, CT is related to international atomic time (TAI) by CT = TAI + 32.184 s.

2. A Natural Example Of Distant Retrograde Orbit Motion

Small bodies in distant retrograde orbits occur naturally throughout our solar system. A well-known example is Saturn's moon Phoebe, about 213 km in diameter [2]. The Saturn-centered orbit of Phoebe has semi-major axis a = 13 million km, period T = 550.31 days, and inclination i = 176° [2]. With respect to the radius of Saturn's gravitational sphere of influence r_{SOI} = 34 million km [4, p. 397], Phoebe has a = 0.38 r_{SOI}.

Numeric simulations of small moons orbiting the Jovian planets [5] indicate escape to interplanetary space will occur in a few decades for prograde orbits with a = 0.5 r_{SOI}. For retrograde orbits, this fate is suffered only at a > 0.7 r_{SOI}. The orbit of Phoebe is therefore thought to be stable over the solar system's age. Escapes from Jovian planets are caused by the *evection resonance*, in which the simulated planet-centered orbit's apoapsis aligns to a sufficient degree and frequency with direction to the Sun. This alignment increases eccentricity e to unity over time and causes escape from the planet. Evection resonances occur less frequently and over shorter time intervals in retrograde orbits than in equivalent prograde orbits.

In this study's SDRO/SDPO context, Earth replaces the Sun as source of the evection resonance. When unstable selenocentric orbits are encountered, the selenocentric "evection angle" ε can be plotted as a function of t to assess the evection resonance's role. The legs defining ε are Earth's selenocentric position $\boldsymbol{r}_E$ and the coasted orbit's osculating Laplacian integral or "eccentricity vector" $\boldsymbol{e}$ pointing to pericynthion with magnitude e. The degree to which ε is near 180° over time will therefore indicate the degree to which evection resonance is contributing to escape from the Moon's vicinity.

Figure 1 coincides with Saturn's equatorial plane and plots the entire 400-year SAT359 Phoebe ephemeris currently available for download [2]. The plot interval is equivalent to 265 Phoebe orbits about Saturn in inertial space. Although the Figure 1 plot interval is 4 times longer than the maximum time interval selected for SDRO stability assessments, Phoebe's T is also nearly 30 times longer than that of any SDRO to be studied. The 265 orbits appearing in Figure 1 are therefore less than the k a stable SDRO or SDPO will tally over 100 years. Nevertheless, Phoebe's example at 0.38 r_{SOI} suggests salient features to expect during SDRO assessments on a similar scale with respect to the Moon's mean r_{SOI} = 66,000 km [6, p. 4].

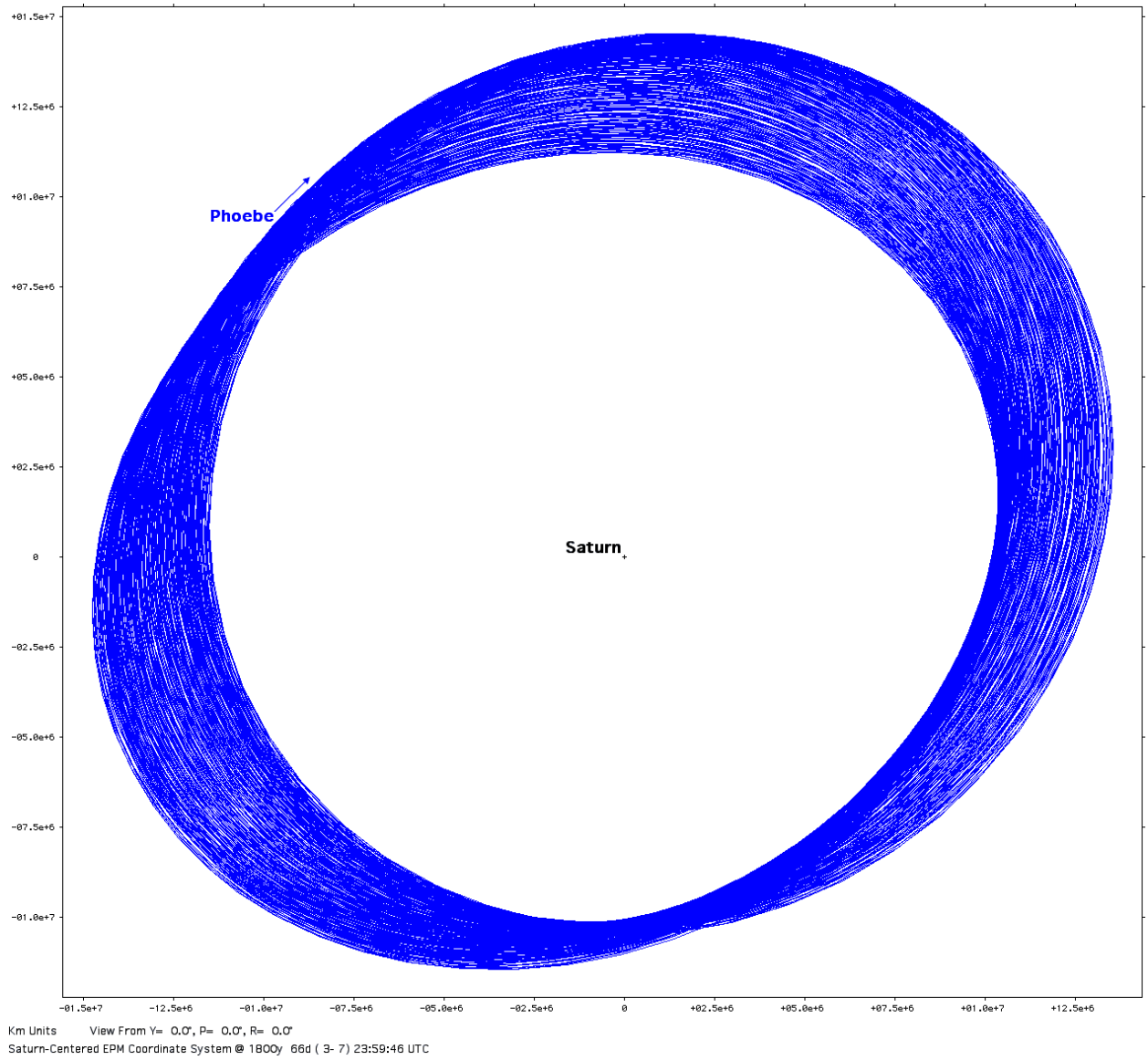

Figure 1. The distant retrograde orbit of Phoebe is plotted with respect to Saturn in that planet's equatorial plane. Motion spans a time interval from year 1800 to year 2200, equivalent to 265 orbits about Saturn in inertial space. The annular envelope encompassing present-day Phoebe orbits is only partially filled during this plot's 400-year time span.

3. Selenocentric Orbits At r_0 = 12,500 km = 0.19 r_{SOI}

At this r_0, $v_0 = \sqrt{\mu / r_0}$ = 0.626278 km/s. Standard SDRO initial conditions with position $+r_0 \boldsymbol{U}$ and velocity $-v_0 \boldsymbol{V}$ are transformed to J2K components as follows, producing initial inclination i_0 = 173.3° with respect to the Moon's equator.

$$\boldsymbol{r}_0 = \begin{bmatrix} +12{,}204.061 \\ +2172.660 \\ +1609.486 \end{bmatrix} \text{ km} \qquad \boldsymbol{v}_0 = \begin{bmatrix} +0.129486 \\ -0.579196 \\ -0.199972 \end{bmatrix} \text{ km/s}$$

A conic T = 34.836 hrs is associated with these initial conditions, and 209 of the standard 600 s integration steps are required to simulate the initial orbit. This SDRO coasts through 100 years without leaving the Moon's vicinity or approaching within 4300 km, tallying k = 25,228. At the start of this coast, a = 12,500 km, and the coast ends with a = 12,419 km, indicating evection resonance effects are negligible.

The 100-year SDRO coast is plotted in Figure 2[§§] as projected onto a selenocentric plane parallel to the epoch J2000.0 ecliptic (J2KE). Figure 2 and similar selenocentric J2KE plots to follow are annotated with two virtually concentric circles about the origin denoting the Moon's surface. Since the Moon's obliquity to the J2000.0 ecliptic is only 6.67° [2], the outer circle is indistinguishable from the Moon's equator. The inner circle is at selenocentric latitude 80° N. Ecliptic longitude is zero at the J2KE plane's ascending node on Earth's mean equator at epoch J2000.0. Known as the first point of Aries (♈), this direction is rightward of the origin in Figure 2 and in all subsequent selenocentric J2KE plots.

[§§] Due to computer memory limitations, the Figure 2 coast actually plotted uses 25 integration steps per orbit, tallies k = 25,228, and ends with a = 12,460 km.

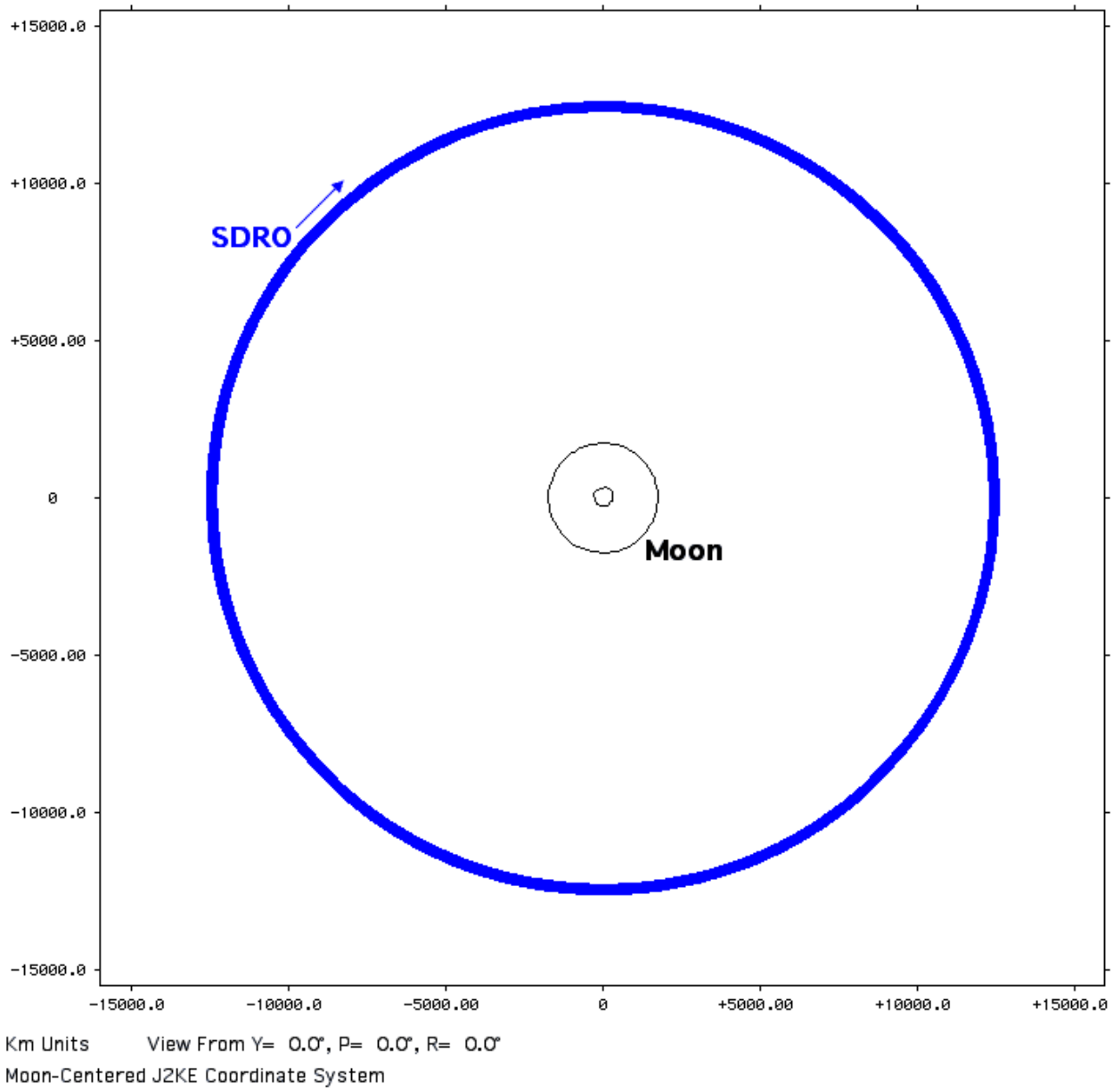

Figure 2. A 100-year SDRO coast with r_0 = 12,500 km and v_0 = 0.626278 km/s is plotted in the selenocentric J2KE plane.

The corresponding SDPO is initialized with position $+r_0\ \boldsymbol{U}$ and velocity $+v_0\ \boldsymbol{V}$, producing i_0 = 6.7° with respect to the Moon's equator. This SDPO coasts through 100 years without leaving the Moon's vicinity or approaching within 4300 km, tallying k = 25,255. At the start of this coast, a = 12,500 km, and the coast ends with a = 12,500 km, indicating evection resonance effects are negligible. Figure 3 is the selenocentric J2KE plot for this SDPO coast[***]. Note the annular envelope encompassing selenocentric motion in Figure 3 is slightly broader than that in Figure 2 (both figures have the same scale to facilitate comparison).

[***] Due to computer memory limitations, the Figure 3 coast actually plotted uses 25 integration steps per orbit, tallies k = 25,255, and ends with a = 12,496 km.

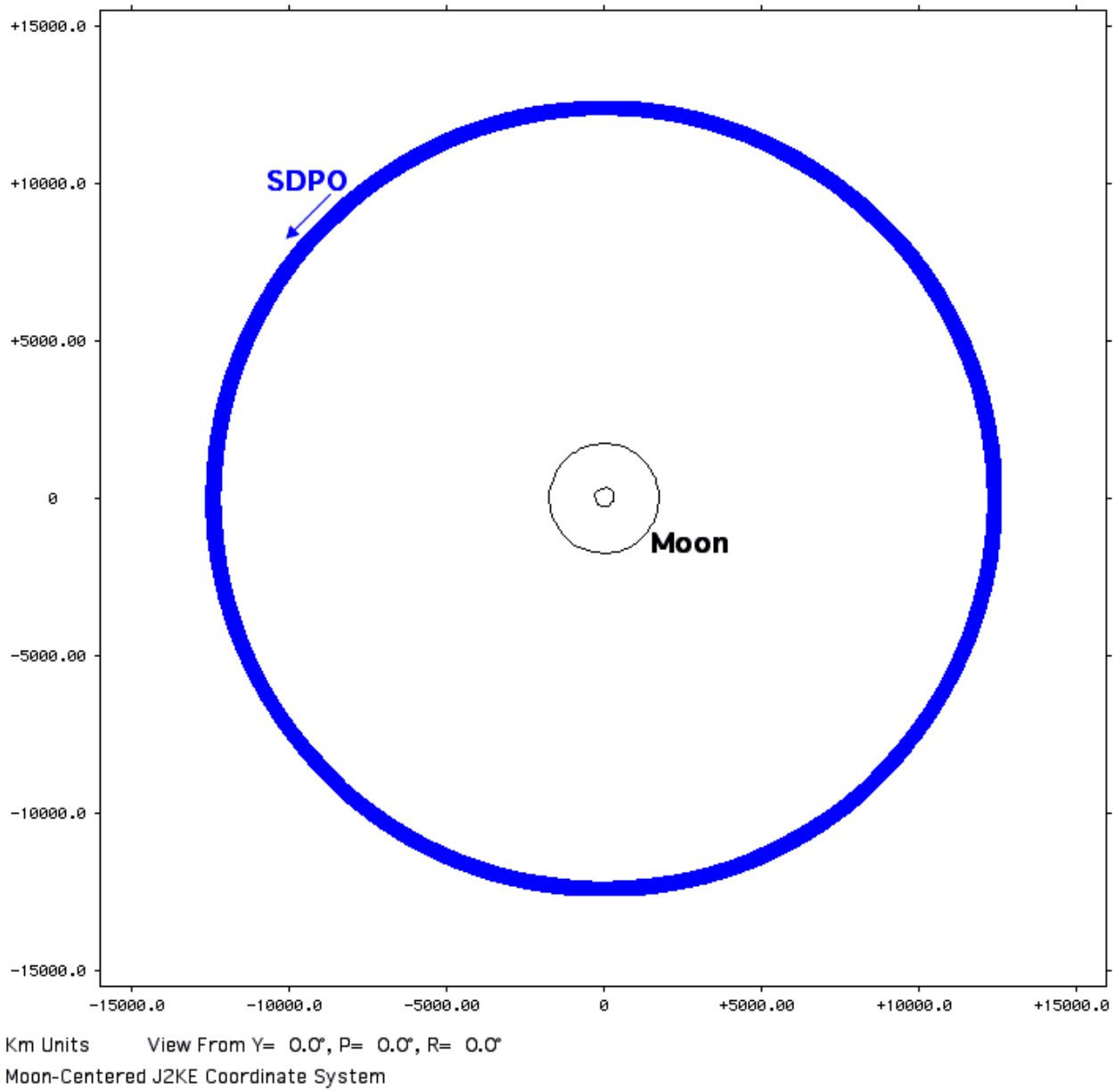

Figure 3. A 100-year SDPO coast with r_0 = 12,500 km and v_0 = 0.626278 km/s is plotted in the selenocentric J2KE plane.

4. Selenocentric Orbits At r_0 = 25,000 km = 0.38 r_{SOI}

Scaled to the Moon's mean r_{SOI} = 66,000 km, Phoebe's orbit would become an SDRO with a = 25,000 km. At r_0 = 25,000 km, $v_0 = \sqrt{\mu / r_0}$ = 0.442845 km/s. Standard SDRO initial conditions with position $+r_0$ ***U*** and velocity $-v_0$ ***V*** are transformed to J2K components as follows, producing initial inclination i_0 = 173.3° with respect to the Moon's equator.

$$\boldsymbol{r}_0 = \begin{bmatrix} +24{,}408.122 \\ +4345.319 \\ +3218.972 \end{bmatrix} \text{ km} \qquad \boldsymbol{v}_0 = \begin{bmatrix} +0.091560 \\ -0.409554 \\ -0.141402 \end{bmatrix} \text{ km/s}$$

A conic $T = 98.530$ hrs is associated with these initial conditions, and 591 of the standard 600 s integration steps are required to simulate the initial orbit. This SDRO coasts through 100 years without leaving the Moon's vicinity or approaching within 4300 km, tallying $k = 9071$. At the start of this coast, $a = 25{,}000$ km, and the coast ends with $a = 24{,}537$ km, indicating evection resonance effects are negligible. Figure 4 is the selenocentric J2KE plot for this SDRO coast[†††].

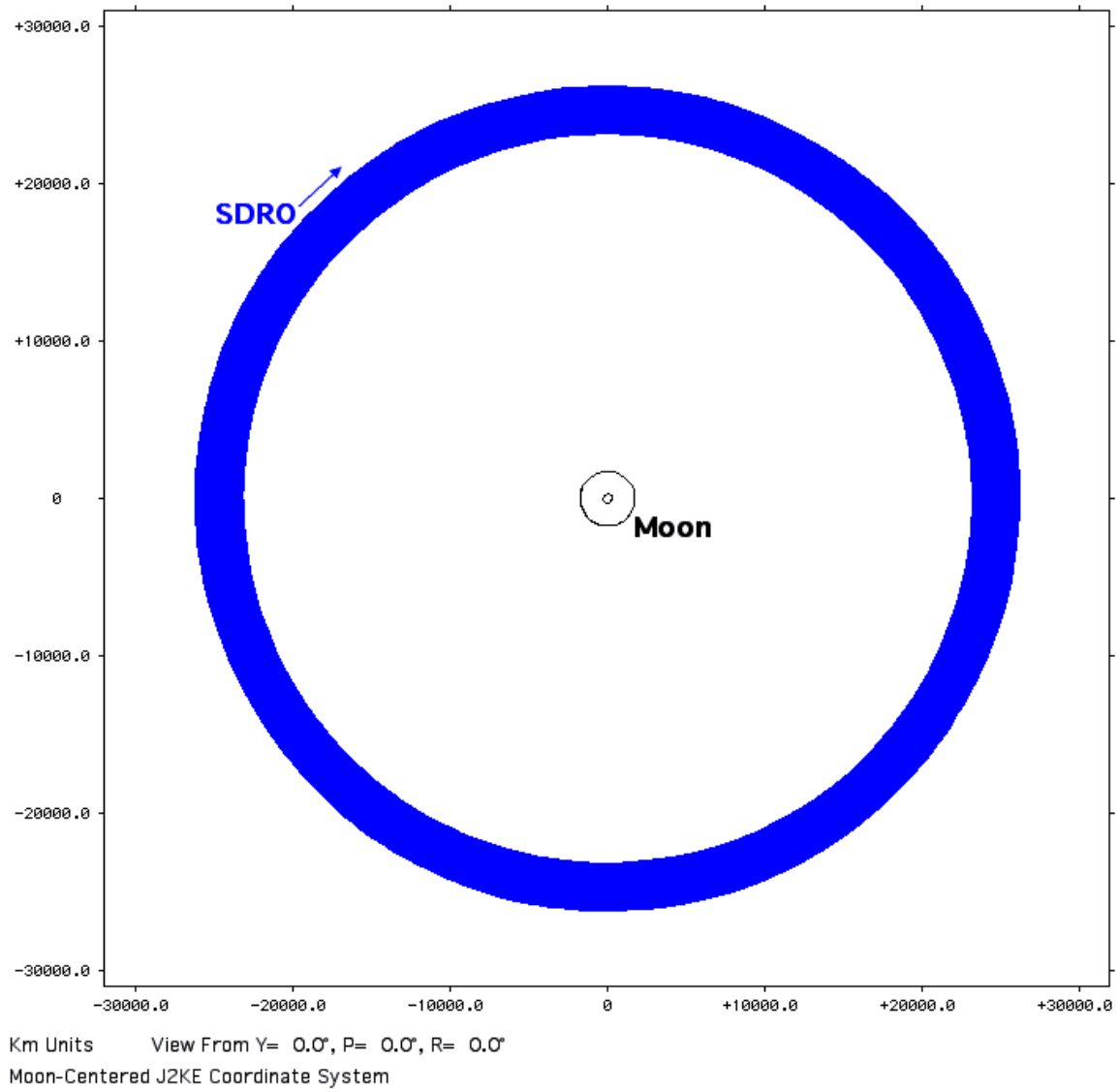

Figure 4. A 100-year SDRO coast with $r_0 = 25{,}000$ km and $v_0 = 0.442845$ km/s is plotted in the selenocentric J2KE plane.

[†††] Due to computer memory limitations, the Figure 4 coast actually plotted uses 60 integration steps per orbit, tallies $k = 9071$, and ends with $a = 24{,}545$ km.

The corresponding SDPO is initialized with position $+r_0$ ***U*** and velocity $+v_0$ ***V***, producing i_0 = 6.7° with respect to the Moon's equator. This SDPO coasts until 17.8 August 2041 CT when it reaches a selenocentric distance less than 4300 km and tallies k = 2541. As this coast terminates, pericynthion height H_P above the Moon's radius of 1737.53 km [2] is +1671 km. Highly unstable motion is evident in the Figure 5 selenocentric J2KE plot for this SDPO coast[‡‡‡].

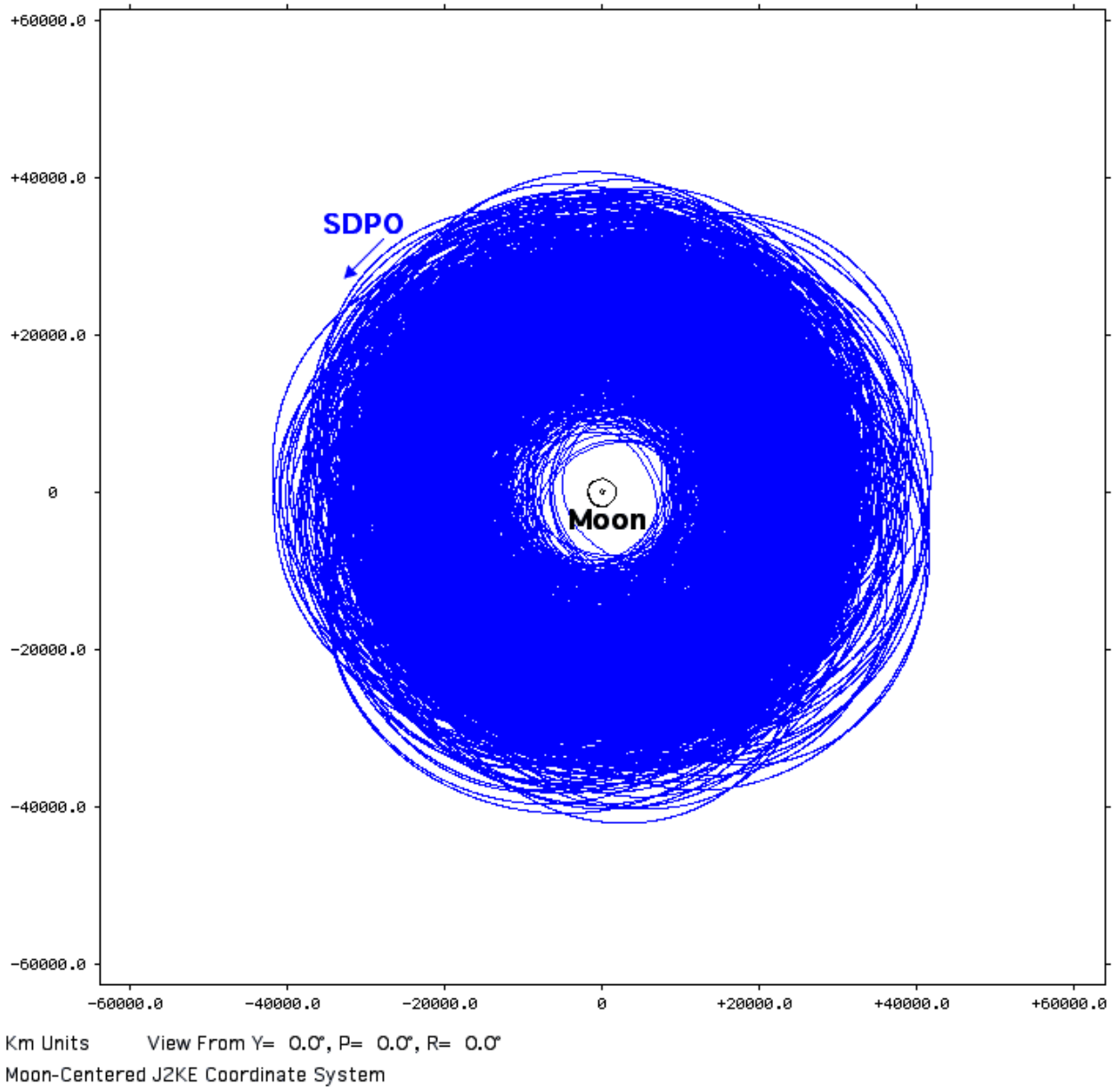

Figure 5. A 12-year SDPO coast with r_0 = 25,000 km and v_0 = 0.442845 km/s is plotted in the selenocentric J2KE plane.

[‡‡‡] Due to computer memory limitations, the Figure 5 coast actually plotted is terminated at 30.5 June 2025 CT using the standard fixed 600 s integration step, tallies k = 1080, and ends with H_P = +17,251 km.

4.1 Evection Resonance In Standard Orbits With r_0 = 25,000 km = 0.38 r_{SOI}

Evection resonance is responsible for contrasting levels of stability evident in Figures 4 and 5. Whereas Figure 4's SDRO motion resides in a well-defined annulus throughout a 100-year coast, SDPO motion in Figure 5 is relatively chaotic over only 12 years. If the SDPO coast were allowed to continue a full 100 years to 2113, a lunar impact or departure from the Moon's vicinity altogether would likely occur at some time after the 17.8 August 2041 CT "close approach" termination epoch.

Adopting the 600 s integration step exclusively, standard SDRO and SDPO initial conditions are each coasted 12 years while selenocentric position and velocity are sampled every 5 days. At each 5-day epoch, $\boldsymbol{e}$ is computed from sampled position and velocity. When $\boldsymbol{e}$ vectors are combined with $\boldsymbol{r}_E$ vectors obtained from [2] at identical epochs, values for ε are obtained. Figures 6 and 7 plot ε and e as functions of t for the SDRO and SDPO coasts, respectively.

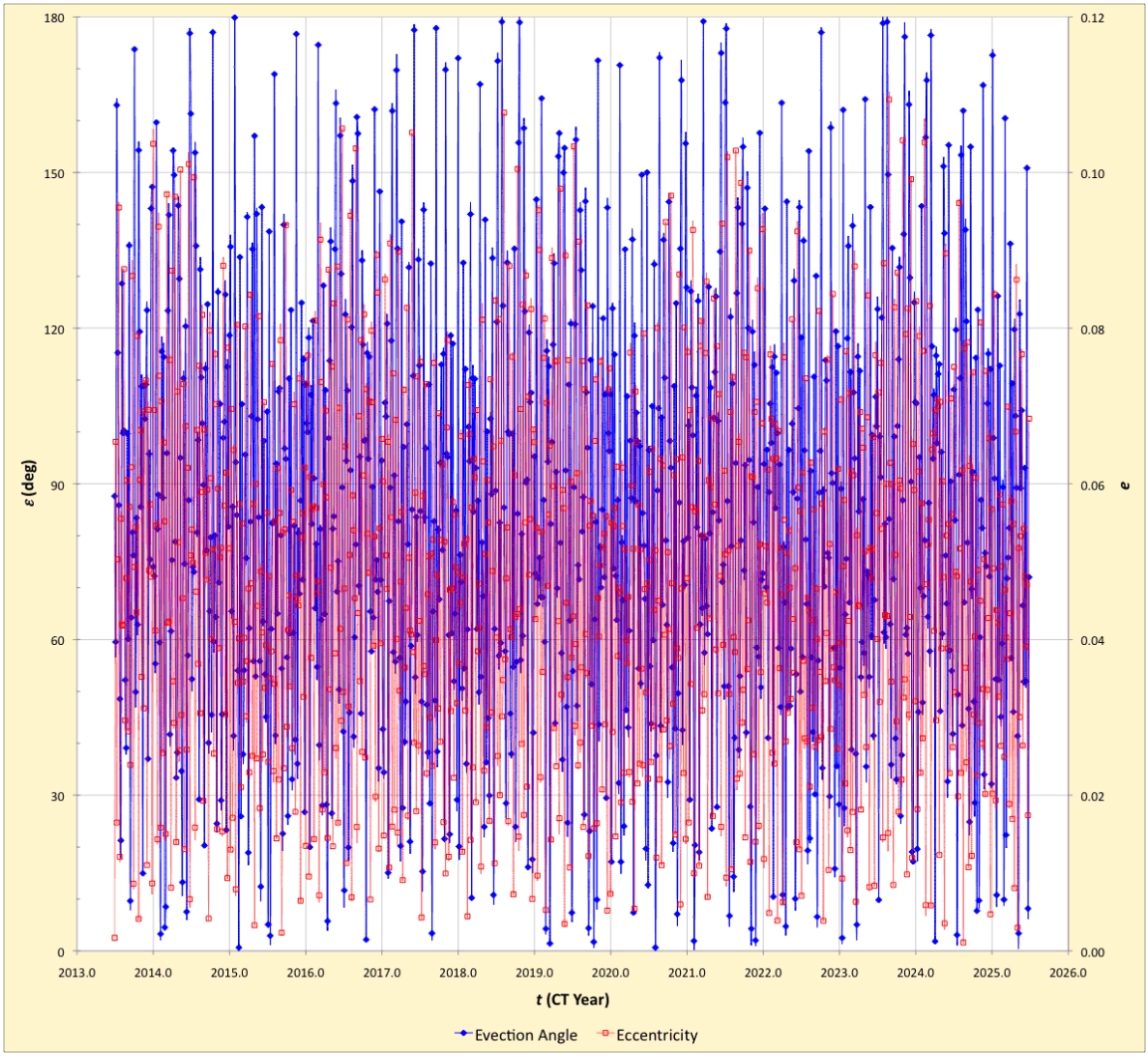

Figure 6. Variations in evection angle ε (filled blue diamonds; scale at left) and eccentricity e (unfilled red squares; scale at right) are plotted for standard SDRO initial conditions with r_0 = 25,000 km and v_0 = 0.442845 km/s as a function of coasted time t.

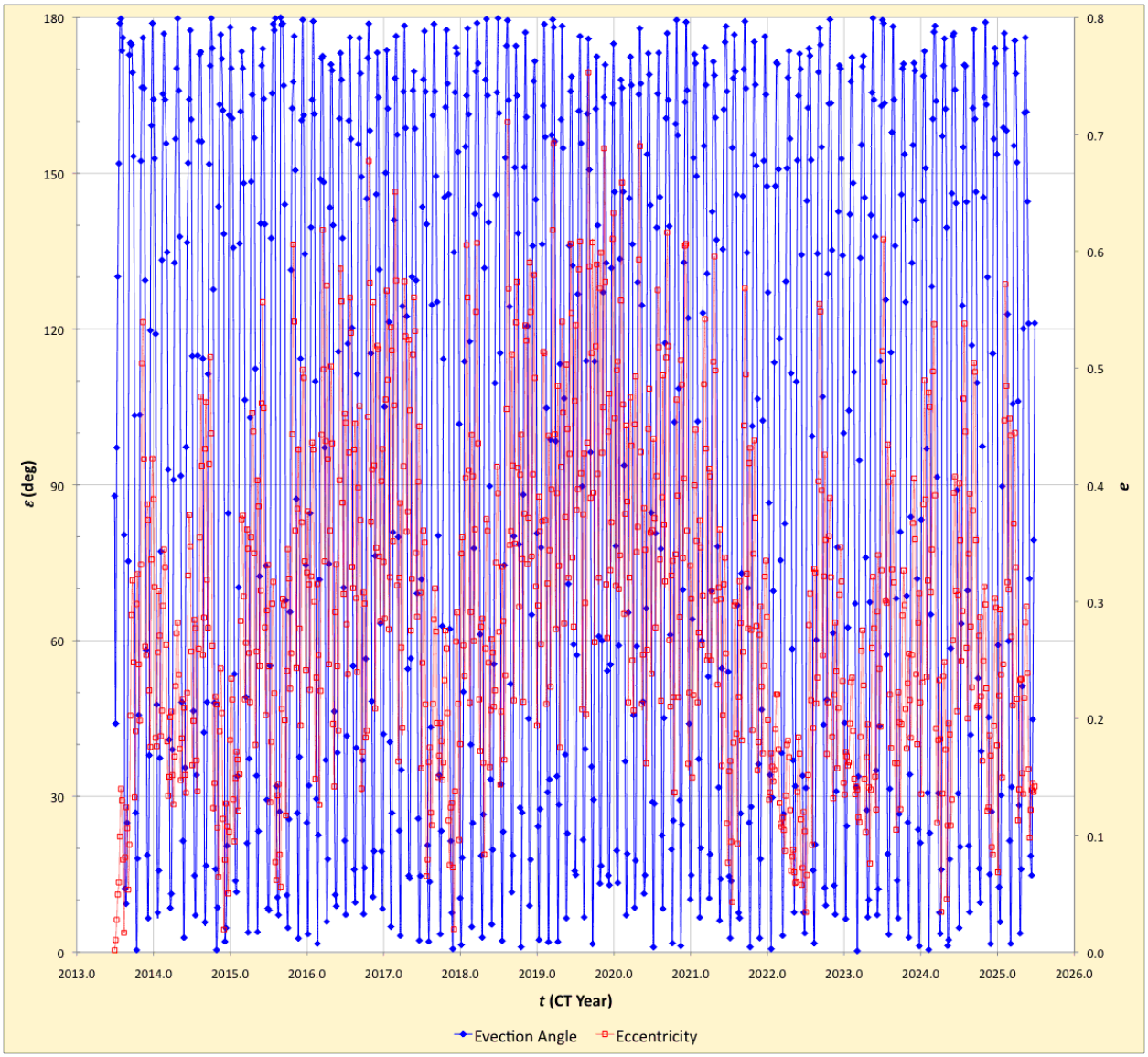

Figure 7. Variations in evection angle ε (filled blue diamonds; scale at left) and eccentricity e (unfilled red squares; scale at right) are plotted for standard SDPO initial conditions with r_0 = 25,000 km and v_0 = 0.442845 km/s as a function of coasted time t.

Two salient differences are evident when comparing Figures 6 and 7. First, variations in e are on completely different scales as indicated by Figure 4 (where SDRO e rarely exceeds 0.1) and Figure 5 (where SDPO e can exceed 0.7 at times). Second, ε values are clustered toward 90° in the SDRO and away from 90° in the SDPO.

As noted earlier, evection is strongest when ε approaches 180°. But clustering among ε data points in Figures 6 and 7 is all but impossible to quantify from visual inspection. Consequently, ε values from these plots are sorted into six 30° "bins". Tallies of the number of values in each bin are recorded in Table 1 for both coasts.

Table 1. The degree to which certain ranges (bins) in evection angle ε are populated during 12-year coasts is quantified with tallies from 877 data points in Figure 6 (SDRO) and 877 data points in Figure 7 (SDPO).

ε Bin (deg)	SDRO Tally	SDPO Tally
0 to 30	108	210
30 to 60	160	105
60 to 90	227	76
90 to 120	203	66
120 to 150	109	123
150 to 180	70	297

In accord with distant retrograde orbit research in other contexts, Table 1 data confirm associated stability theory's dependence on effects of the evection resonance. This resonance contributes most to orbit instability in the 150° to 180° ε bin. The same bin is most lightly populated by SDRO data and most heavily populated by SDPO data.

4.2 Differential Corrections To The r_0 = 25,000 km = 0.38 r_{SOI} SDPO

As suggested in Section 1, two types of boundary conditions are applied to differential corrections of the r_0 = 25,000 km SDPO documented in Section 4. Both types specify selenocentric position $+r_0$ $\boldsymbol{U}$ at $t = 0$. But a half-rev differential correction specifies selenocentric position $-r_0$ $\boldsymbol{U}$ at $t = t_1$, whereas a one-rev differential correction specifies selenocentric position $+r_0$ $\boldsymbol{U}$ at $t = t_1$. The two boundary condition types are also distinguished by the values of t_1 with which they are associated. Half-rev differential correction iterations each have t_1 near 0.5 T (about 2 days), and one-rev differential correction iterations each have t_1 near T (about 4 days).

Half-rev differential corrections to the r_0 = 25,000 km SDPO with $|\gamma_0|$ and $|\gamma_1|$ less than 10° are obtained over the interval from 2.0 days $\leq t_1 \leq$ 3.0 days. When assessed for stability, all half-rev v_0' coasts either depart the Moon's vicinity or approach within 4300 km before year 2015. These results exhibit less stability than does the corresponding uncorrected v_0 coast plotted in Figure 5. For half-rev differential corrections to offer improved stability over the v_0 coast requires selenocentric distance r_1 along $-\boldsymbol{U}$ at $t = t_1$ also be iterated to an optimal value near 21,000 km when t_1 is near 2.6 days.

The additional r_1 iteration is not necessary for one-rev differential corrections to achieve stable 100-year coasts. This is apparently because a closed orbit (with $r_0 = r_1$ in a one-rev context) offers near-maximum stability at any t_1 near T. With one-rev differential corrections producing stability equivalent to more complex half-rev iterations, only the former are documented hereafter.

Table 2. One-rev differential corrections to the SDPO with r_0 = 25,000 km and v_0 = 0.442845 km/s are listed in order of increasing t_1. When coasted, every one of these corrected SDPOs remains in the Moon's vicinity for 100 years without approaching closer than 4300 km. The degree of differential correction is quantified by the vector difference magnitude $\Delta v_{DC} = |v_0' - v_0|$.

t_1 (hrs)	γ_0 (deg)	γ_1 (deg)	k	Δv_{DC} (km/s)
78	+11.507	-11.354	16,074	0.141350
84	+6.910	-6.792	14,314	0.098986
90	+4.578	-4.530	13,056	0.071872
96	+3.087	-3.125	12,045	0.051669
102	+2.048	-2.179	11,245	0.035742
108	+1.297	-1.521	10,509	0.022808
114	+0.749	-1.062	9899	0.012128
120	+0.354	-0.750	9327	0.003515

Table 2 very nearly spans the range of all one-rev t_1 values giving rise to stable 100-year coasts for r_0 = 25,000 km SDPOs. At t_1 = 72 hrs, γ_0 = +71.150° causes coasted selenocentric distance to fall below 4300 km at 3.4 July 2013 CT with k = 0. At t_1 = 123 hrs, γ_0 = +0.203° is smaller than any γ_0 value in Table 2, but coasted selenocentric distance falls below 4300 km at 5.8 September 2053 CT with k = 3622. By virtue of its minimal k = 9327 among Table 2's 100-year coasts, the t_1 = 120 hrs differential correction is considered the most stable SDPO with r_0 = 25,000 km. A selenocentric plot of this coast's trajectory appears in Figure 8[§§§]. The associated selenocentric J2K initial conditions are as follows.

$$\boldsymbol{r}_0 = \begin{bmatrix} +24{,}408.122 \\ +4345.319 \\ +3218.972 \end{bmatrix} \text{ km} \qquad \boldsymbol{v}_0' = \begin{bmatrix} -0.088450 \\ +0.407933 \\ +0.141169 \end{bmatrix} \text{ km/s}$$

[§§§] Due to computer memory limitations, the Figure 8 coast actually plotted is terminated at 30.5 June 2025 CT using the standard fixed 600 s integration step, tallies k = 1120, and ends with H_P = +18,582 km.

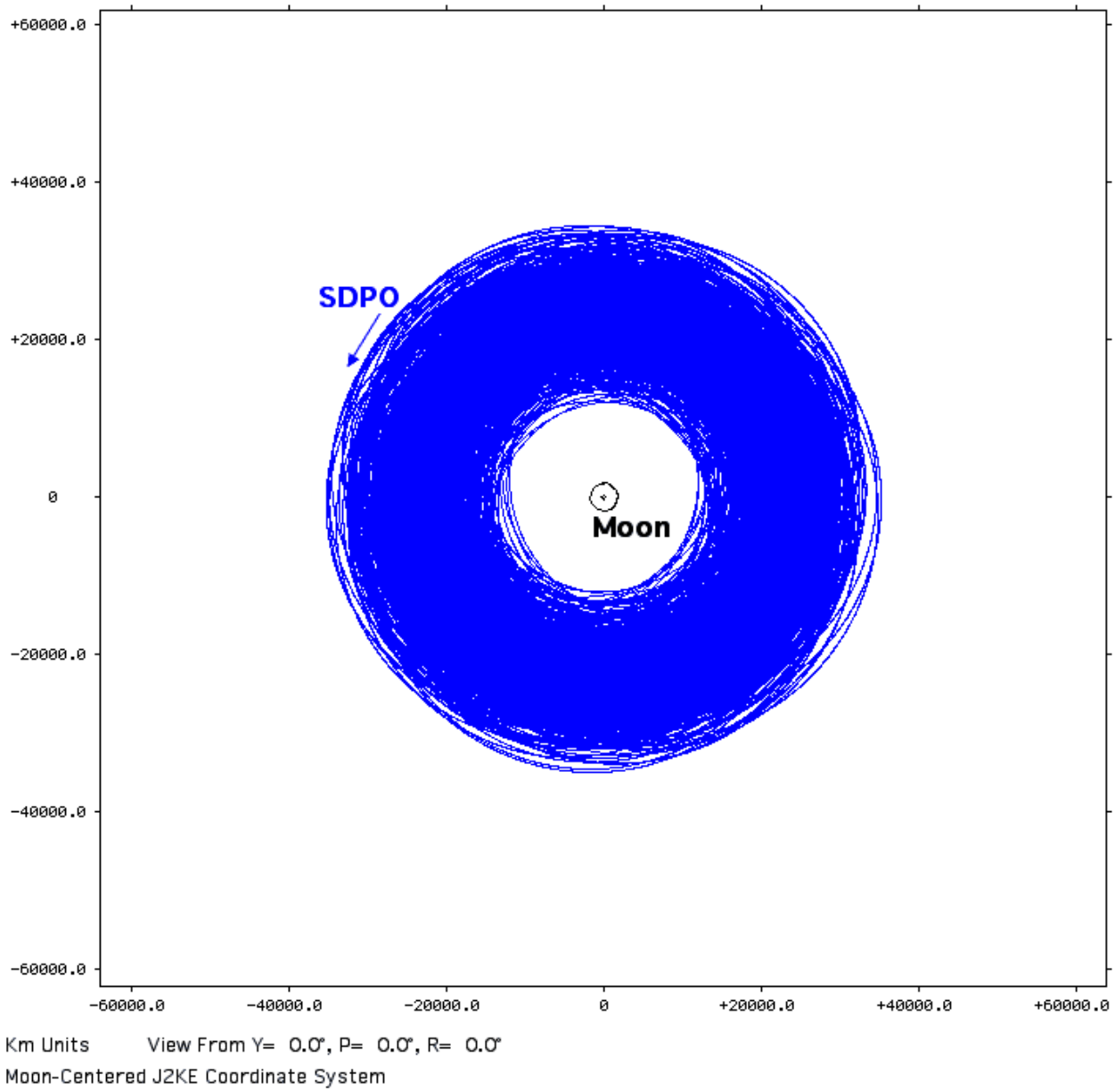

Figure 8. A 12-year SDPO coast with r_0 = 25,000 km and differentially corrected v_0' = 0.440638 km/s is plotted in the selenocentric J2KE plane.

Compared with the uncorrected SDPO coast plotted in Figure 5, the Figure 8 coast indicates increased stability, but it cannot approach the enhanced stability of the uncorrected SDRO coast in Figure 4. Evection resonance characteristics associated with the differentially corrected Figure 8 coast, as plotted in Figure 9, more closely resemble the uncorrected SDPO (see Figure 7) than they do the uncorrected SDRO (see Figure 6). However, Figure 9 generally enjoys reduced e values with respect to Figure 7. Reduced e lessens the effects of evection in the differentially corrected coast and imparts enhanced stability vice the uncorrected SDPO. In Figure 9, note how ε tends to freeze at elevated values when e is near zero. Because the coasted semi-major axis is poorly defined at times when e is near zero, ε near 180° is likely a consequence of Earth gravity perturbations tending to align apocynthion with -$\boldsymbol{U}$.

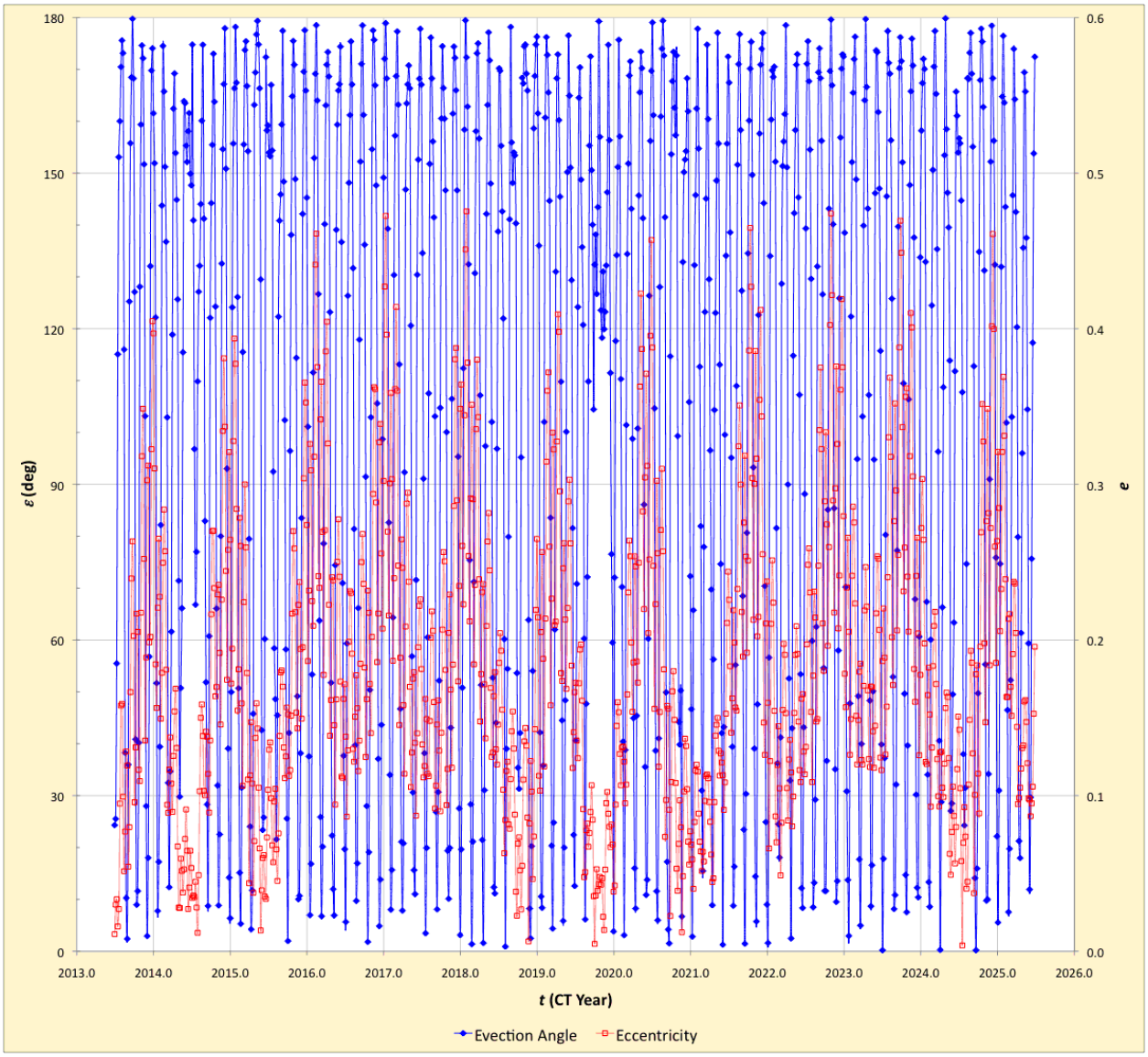

Figure 9. Variations in evection angle ε (filled blue diamonds; scale at left) and eccentricity e (unfilled red squares; scale at right) are plotted for differentially corrected SDPO initial conditions with r_0 = 25,000 km and v_0' = 0.440638 km/s as a function of coasted time t.

Table 3 adds ε bin tallies from Figure 9 to those already presented in Table 1 from Figures 6 and 7. The bimodal character in both SDPO tallies is in contrast to ε values concentrated near 90° in the single SDRO tally.

Table 3. The degree to which certain ranges (bins) in evection angle ε are populated during 12-year coasts from r_0 = 25,000 km is quantified with tallies from 877 data points in each of Figures 6, 7, and 9 (left to right).

ε Bin (deg)	Uncorrected SDRO Tally	Uncorrected SDPO Tally	Corrected SDPO Tally
0 to 30	108	210	157
30 to 60	160	105	121
60 to 90	227	76	69
90 to 120	203	66	82
120 to 150	109	123	143
150 to 180	70	297	305

5. Selenocentric Orbits At r_0 = 70,000 km = 1.06 r_{SOI}

At r_0 = 70,000 km, $v_0 = \sqrt{\mu / r_0}$ = 0.264651 km/s. Standard SDRO initial conditions with position $+r_0$ $\boldsymbol{U}$ and velocity $-v_0$ $\boldsymbol{V}$ are transformed to J2K components as follows, producing initial inclination i_0 = 173.3° with respect to the Moon's equator.

$$\boldsymbol{r}_0 = \begin{bmatrix} +68{,}342.741 \\ +12{,}166.894 \\ +9013.122 \end{bmatrix} \text{ km} \qquad \boldsymbol{v}_0 = \begin{bmatrix} +0.054718 \\ -0.244755 \\ -0.084504 \end{bmatrix} \text{ km/s}$$

A conic T = 19.235 days is associated with these initial conditions, and 2770 of the standard 600 s integration steps are required to simulate the initial orbit. This SDRO coasts through 22 days without leaving the Moon's vicinity until it approaches within 4300 km, tallying k = 1. At the start of this coast, a = 70,000 km, and the coast ends with $a < 0$ and H_P = -124 km, indicating evection resonance effects are appreciable. Figure 10 is the selenocentric J2KE plot for this brief SDRO coast. The plot offers only vague and fleeting resemblances to various conic trajectories. Differential corrections supported by CRTBP theory will therefore be necessary to achieve stable selenocentric motion over 100-year coasts from r_0 = 70,000 km.

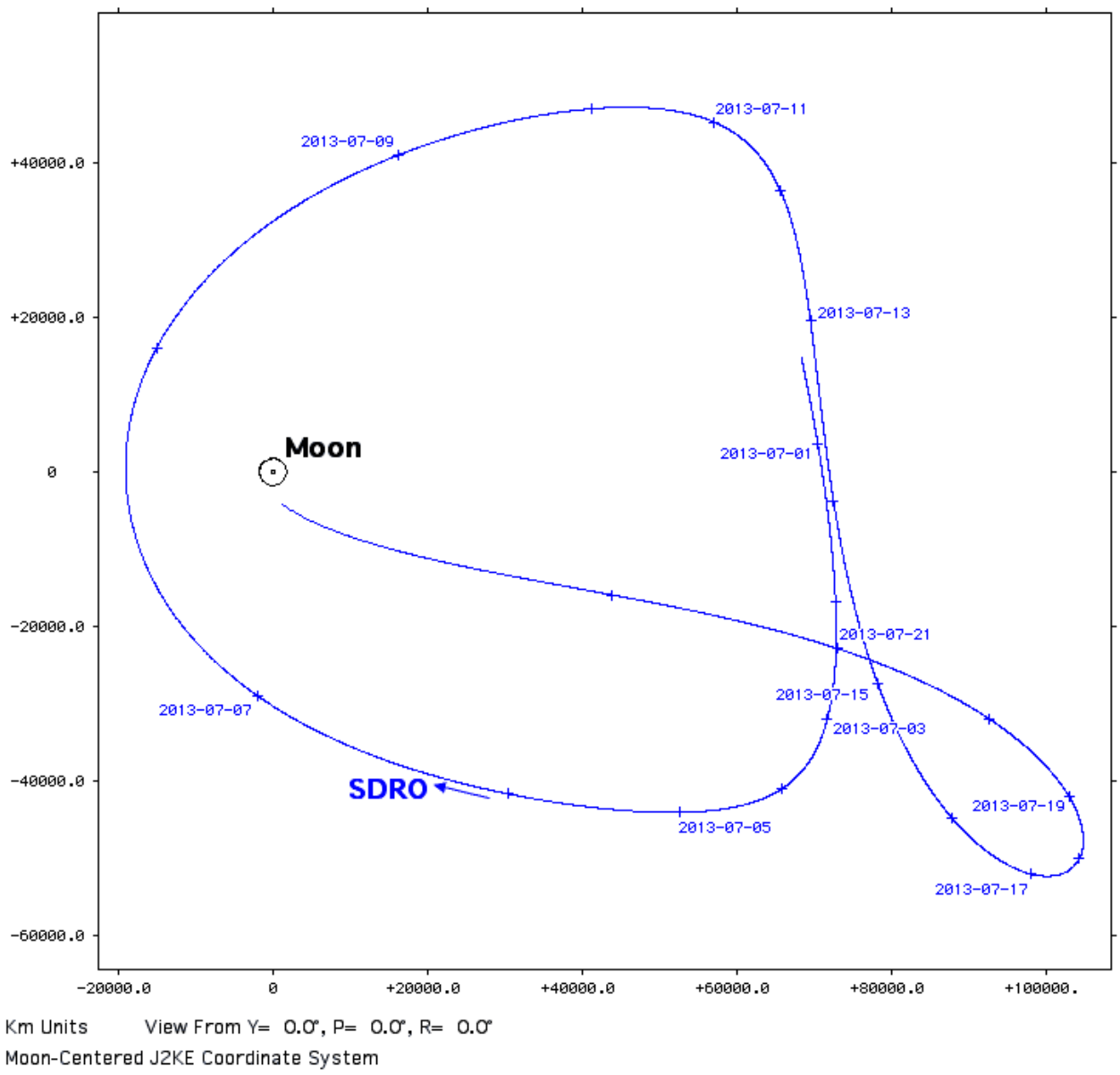

Figure 10. A 22-day SDRO coast with r_0 = 70,000 km and v_0 = 0.264651 km/s is plotted in the selenocentric J2KE plane starting at 30.5 June 2013 CT. Ticks are at 00:00 CT and annotated with calendar date in YYYY-MM-DD format every 2 days.

The corresponding SDPO is initialized with position $+r_0$ ***U*** and velocity $+v_0$ ***V***, producing i_0 = 6.7° with respect to the Moon's equator. During coast, this SDPO immediately departs the Moon's vicinity, tallying $k = 0$. Recalling the marginally stable results of differential corrections applied to an r_0 = 25,000 km SDPO as documented in Section 4.2, a similar effort at r_0 = 70,000 km is considered to be of insufficient interest. Differential corrections to the r_0 = 70,000 km SDRO therefore occupy the remainder of this section.

From Section 4.2 experience, differential corrections to the r_0 = 70,000 km SDRO rely on one-rev boundary conditions with selenocentric position $+r_0$ ***U*** at $t = 0$ and $t = t_1$. Figure 10 suggests that, for selenocentric velocity near $-v_0$ ***V*** at $t = 0$, one-rev boundary conditions will tend to be

satisfied near t_1 = 13 days when selenocentric distance is very nearly r_0. Per data in Table 4, differentially corrected SDRO stability does indeed appear to be near its maximum at that coast time.

Table 4. One-rev differential corrections to the SDRO with r_0 = 75,000 km and v_0 = 0.264651 km/s are listed in order of increasing t_1. Values for k apply to the stability assessment coast's terminal epoch. The degree of differential correction is quantified by the vector difference magnitude $\Delta v_{DC} = |v_0' - v_0|$.

t_1 (days)	γ_0 (deg)	γ_1 (deg)	k	Δv_{DC} (km/s)	Terminal Coast Condition
12.25	-6.886	+5.875	448	0.058031	Depart Moon 24.0 Dec 2039 CT
12.50	-5.768	+4.726	807	0.055249	Depart Moon 30.3 Apr 2060 CT
12.75	-4.664	+3.598	1472	0.052970	t = 100 years
13.00	-3.573	+2.494	1457	0.051237	t = 100 years
13.25	-2.493	+1.412	1431	0.050090	Lunar dist. < 4300 km 7.0 Sep 2111
13.50	-1.422	+0.356	85	0.049553	Depart Moon 28.0 May 2019 CT

By virtue of its minimal k = 1457 among Table 4's 100-year coasts, the t_1 = 13.00 days differential correction is considered the most stable SDRO with r_0 = 70,000 km. A selenocentric plot of this coast's initial 28 days appears in Figure 11 for comparison to uncorrected motion in Figure 10. Selenocentric J2K initial conditions associated with Figure 11 are as follows.

$$\boldsymbol{r}_0 = \begin{bmatrix} +68{,}342.741 \\ +12{,}166.894 \\ +9013.122 \end{bmatrix} \text{ km} \qquad \boldsymbol{v}_0' = \begin{bmatrix} +0.045529 \\ -0.291773 \\ -0.102673 \end{bmatrix} \text{ km/s}$$

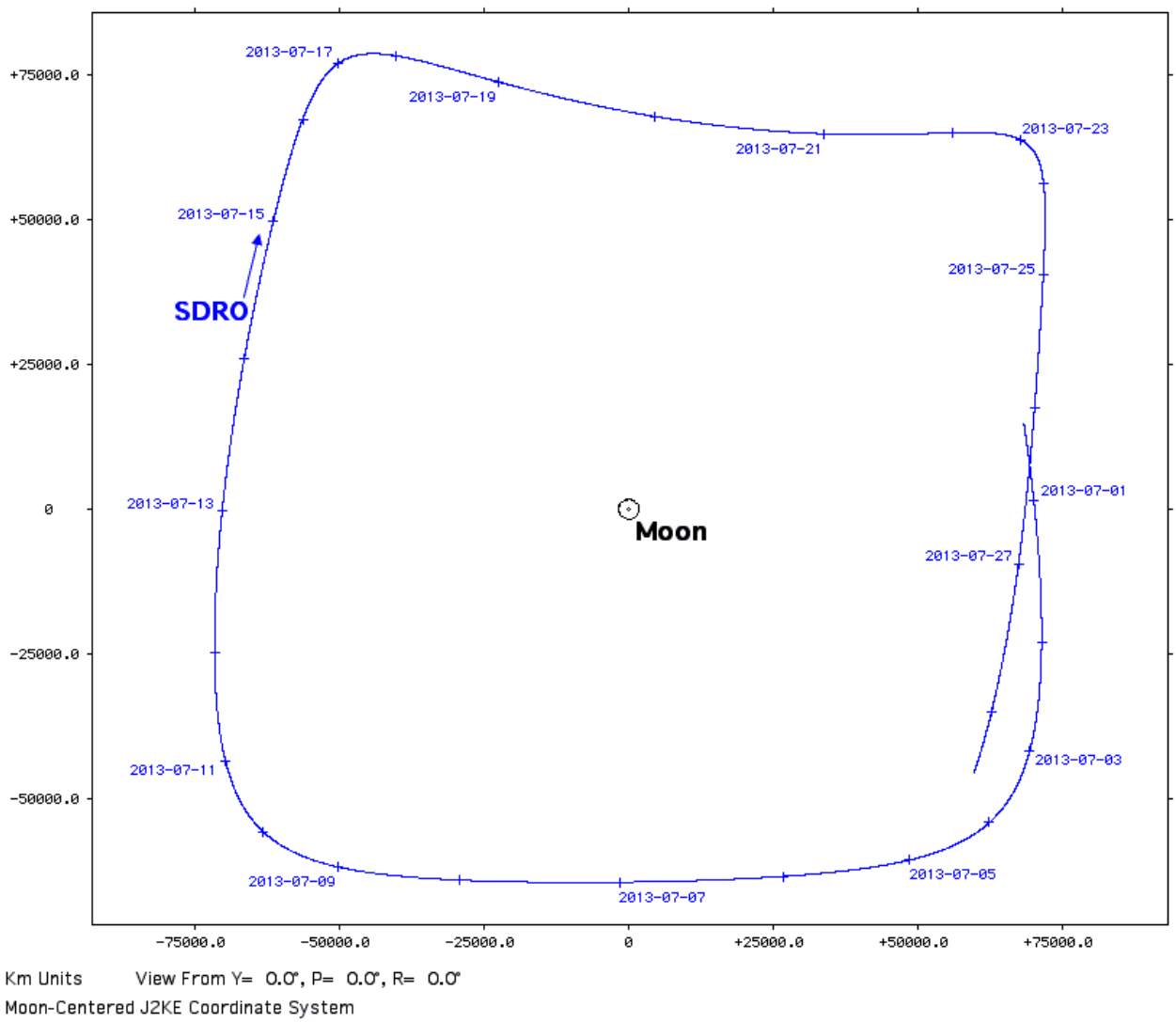

Figure 11. A 28-day differentially corrected SDRO coast with r_0 = 70,000 km and v_0' = 0.312644 km/s is plotted in the selenocentric J2KE plane starting at 30.5 June 2013 CT. This is the first month of a coast staying in the Moon's vicinity for 100 years without approaching closer than ~60,000 km (see Figure 13). Ticks are at 00:00 CT and annotated with calendar date in YYYY-MM-DD format every 2 days.

The Figure 11 trajectory might be described as a "lazy square" in selenocentric inertial space, and it bears little resemblance to conic motion. Figure 12 plots the same trajectory in geocentric inertial space. Along with illustrating the exotic character of SDRO motion from a geocentric perspective, Figure 12 provides insight regarding SDRO stability and SDPO instability at r_0 = 70,000 km. One-rev differential correction boundary conditions for this r_0 require the coasted trajectory to be 70,000 km outside the Moon's orbit on 30.5 June 2013 CT and again about 13 days later. During this interval, the Moon has completed almost half a geocentric inertial orbit. To be in any kind of equilibrium with the Moon's geocentric orbit, the SDPO must lie about 70,000 km Earthward from the Moon at some point during the 13-day interval. But posigrade motion with respect to the Moon on 30.5 June 2013 CT, together with γ_0 near zero, preclude

crossing the Moon's orbit and doom the SDPO to departing the Moon's vicinity even if one-rev boundary conditions can be satisfied.

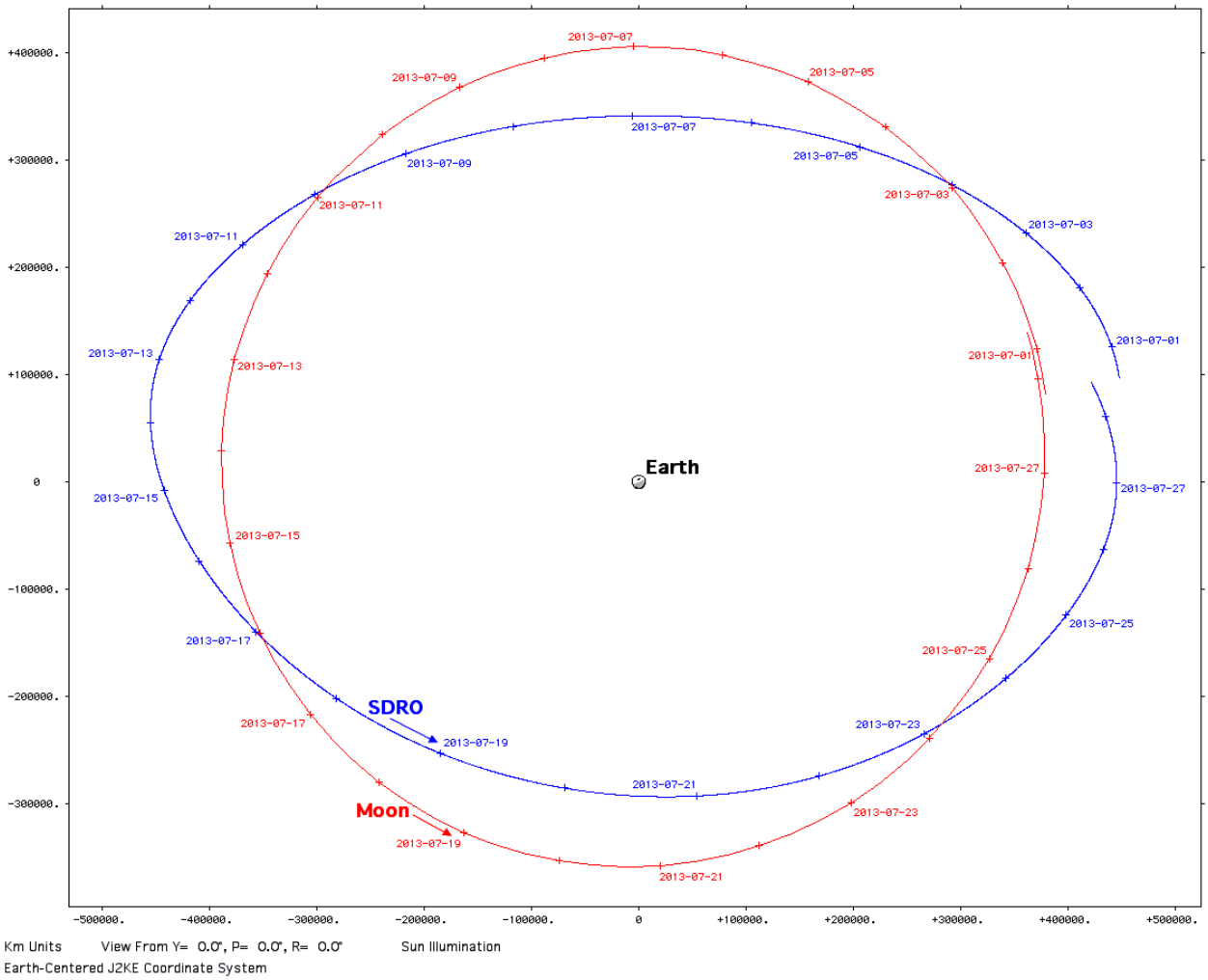

Figure 12. A 28-day differentially corrected SDRO coast with r_0 = 70,000 km and v_0' = 0.312136 km/s is plotted in the geocentric J2KE plane starting at 30.5 June 2013 CT. Ticks are at 00:00 CT and annotated with calendar date in YYYY-MM-DD format every 2 days. The shaded area is Earth's nightside.

A more extended plot of SDRO coast with r_0 = 70,000 km and v_0' = 0.312644 km/s appears in Figure 13[****].

[****] Due to computer memory limitations, the Figure 13 coast actually plotted uses fixed 7200 s integration steps and tallies k = 1457.

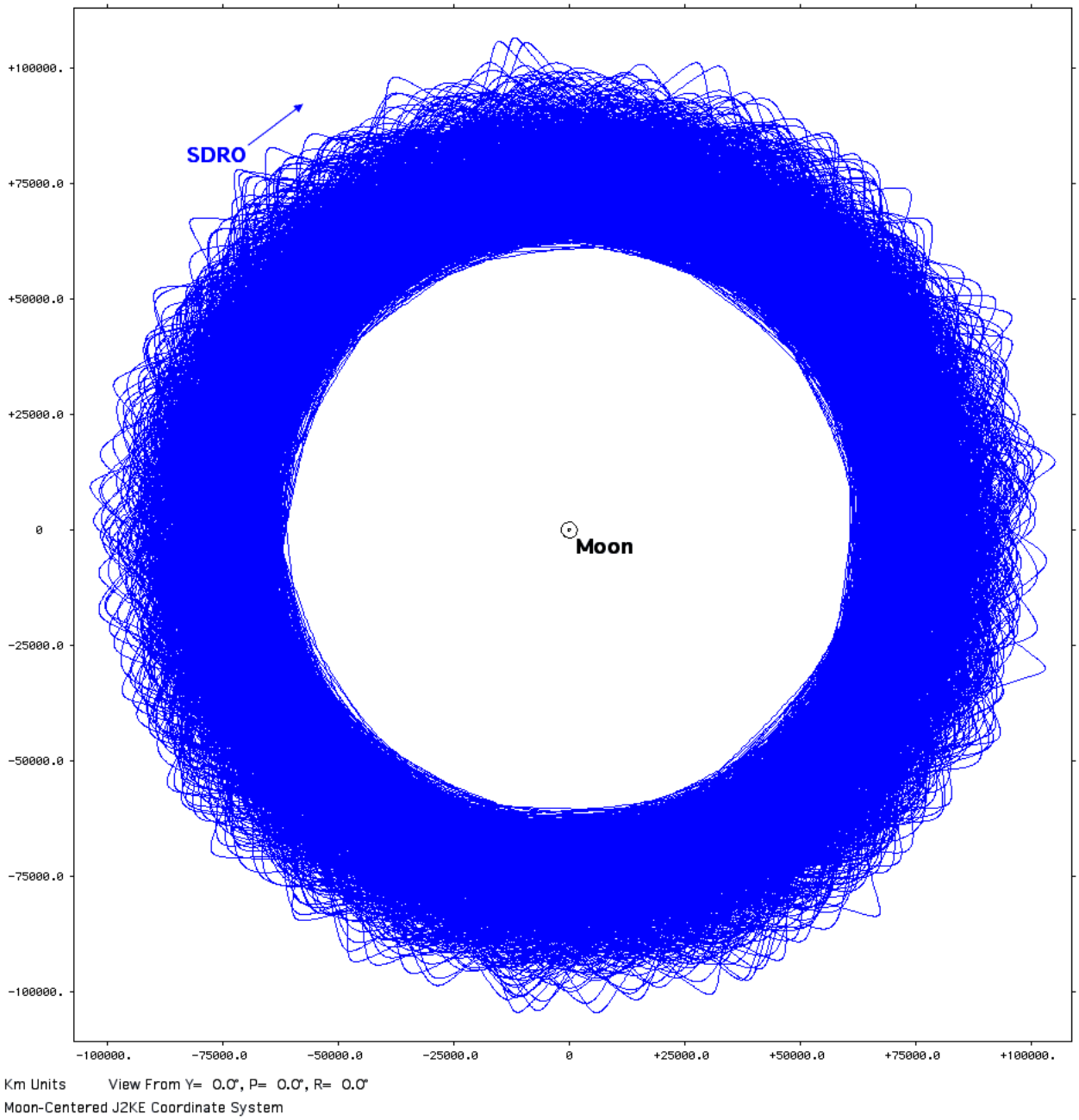

Figure 13. A 100-year SDRO coast with r_0 = 70,000 km and differentially corrected v_0' = 0.312644 km/s is plotted in the selenocentric J2KE plane.

Evection resonance characteristics associated with the differentially corrected coast in Figures 11 through 13 are plotted in Figure 14. Note the heavy concentration of ε values near 90° in Figure 14, a condition consistent with stability in CRTBP theory. This concentration is quantified in Table 5.

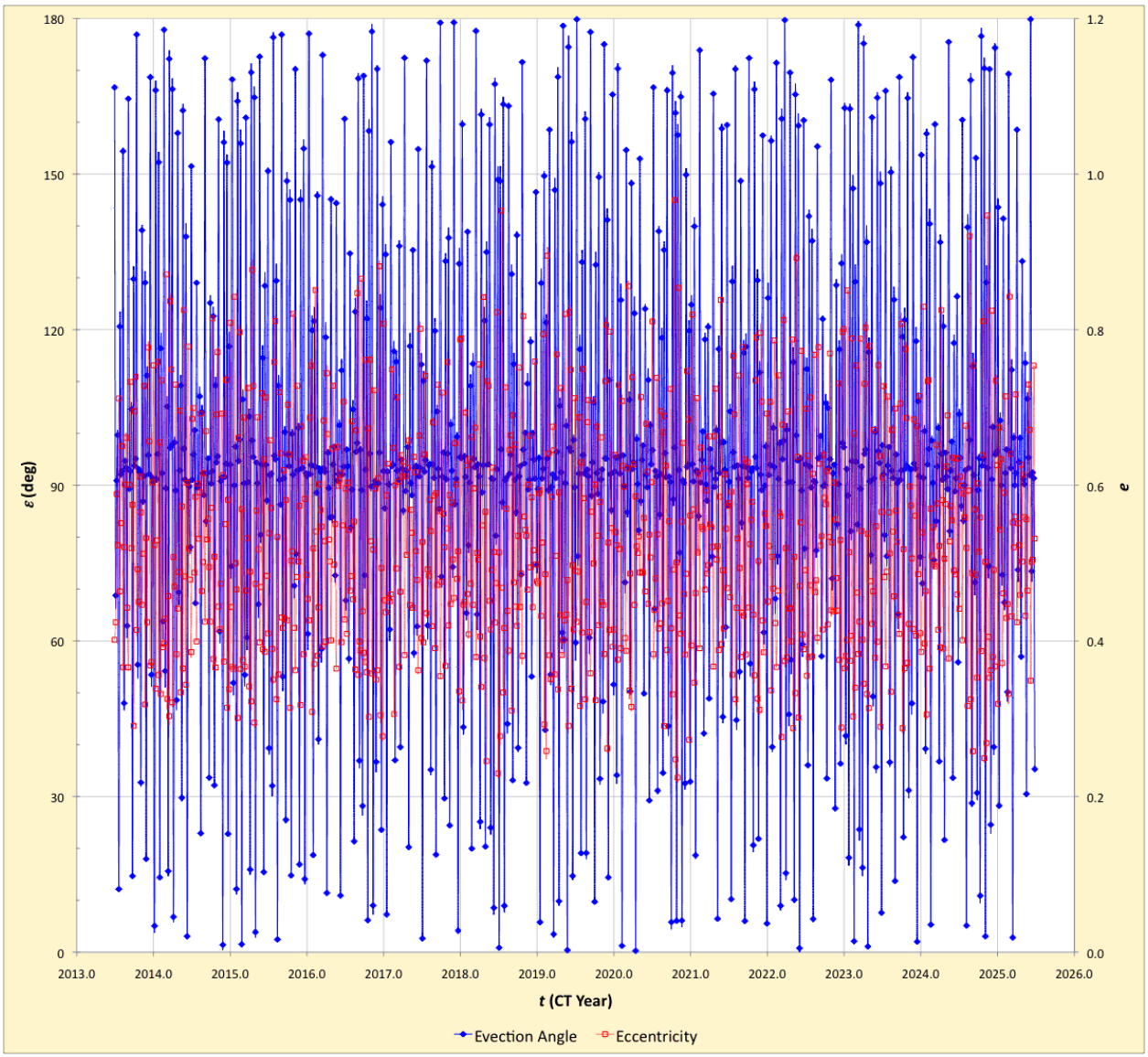

Figure 14. Variations in evection angle ε (filled blue diamonds; scale at left) and eccentricity e (unfilled red squares; scale at right) are plotted for differentially corrected SDRO initial conditions with r_0 = 70,000 km and v_0' = 0.312644 km/s as a function of coasted time t.

Table 5. The degree to which certain ranges (bins) in evection angle ε are populated in Figure 14 is quantified with tallies from its 877 data points.

ε Bin (deg)	SDRO Tally
0 to 30	90
30 to 60	72
60 to 90	122
90 to 120	401
120 to 150	78
150 to 180	114

6. Conclusions

A series of coasted trajectory simulations at initial selenocentric distances r_0 = 12,500 km, 25,000 km, and 70,000 km has been conducted with accelerations from Earth, Sun, and Moon gravity. As r_0 increases, very nearly circular trajectories become progressively more exotic and inherently less stable as Earth and Sun perturbations grow in importance. Variations in selenocentric distance to which these trajectories are confined, together with a tally of lunar equator crossings, have been demonstrated as effective orbit stability metrics.

Application of CRTBP theory in the Earth-Moon system provides additional insight to simulation stability. Evection resonance from this theory, in which the selenocentric Laplacian integral of conic motion tends to align with selenocentric Earth position, has been shown to strongly correlate with coasted trajectory stability. In addition, stable trajectories do indeed tend to cross the $V = 0$ plane almost orthogonally in general accord with CRTBP theory. This necessary condition provides guidance in selecting simulation initial conditions for further stability assessment. The Moon's mean geocentric orbit eccentricity is 0.05490 [2] and is thought to be chief among causes responsible for minor deviations from CRTBP theory documented in this paper.

Simulations at each r_0 have demonstrated the degree to which retrograde motion is inherently more stable than prograde motion. Evection resonance is shown to be stronger in prograde trajectories with respect to their retrograde counterparts. This tendency is predicted by CRTBP theory and is observed in natural satellites orbiting large planets of our solar system such as Saturn's moon Phoebe.

This paper's scope has been limited with respect to possible selenocentric orbits being targeted by ARM. First, all initial conditions are at the epoch 2013 June 30.5 CT, when the Moon's orbit has a geocentric true anomaly of 113.105° [2]. Given the chaotic nature of motion at larger r_0 values explored by this paper, significantly different results should be expected for initial conditions at other epochs. Second, all initial conditions are very close to the Moon's geocentric orbit plane. Depending on approach geometry from interplanetary space, along with intermediate lunar gravity assists, ARM's final selenocentric orbit may be appreciably inclined to the Moon's geocentric orbit plane. Finally, perturbations such as solar radiation pressure may be highly relevant to ARM's selenocentric orbit stability over decades of time. Such perturbations are not modeled in this paper's simulations.

Despite the foregoing limitations, this paper does indicate the precision with which ARM must achieve selenocentric orbit near r_0 = 70,000 km. Data from Table 4 imply initial velocity required to achieve 100-year stability must be imparted to a precision of about 0.005 km/s.

References

[1] Adamo, D. R., "A Precision Orbit Predictor Optimized For Complex Trajectory Operations," *Astrodynamics 2003, Advances in the Astronautical Sciences*, Vol. 116, Univelt, San Diego, CA, 2003, pp. 2567-2586.

[2] Giorgini, J. D., Yeomans, D. K., Chamberlin, A. B., Chodas, P. W., Jacobson, R. A., Keesey, M. S., Lieske, J. H., Ostro, S. J., Standish, E. M., Wimberly, R. N., "JPL's On-Line Solar System Data Service", *Bulletin of the American Astronomical Society*, Vol. 28, No. 3, p. 1158, 1996.[††††]

[3] Parker, J.S. and Anderson, R. L., *Low-Energy Lunar Trajectory Design*, JPL, 2013.[‡‡‡‡]

[4] Battin, R. H., *An Introduction to the Mathematics and Methods of Astrodynamics*, AIAA, 1987.

[5] Nesvorný, D., Alvarellos, J. L. A., Dones, L., Levison, H. F., "Orbital And Collisional Evolution Of The Irregular Satellites", *The Astronomical Journal*, Vol. 126, No. 7, The American Astronomical Society, 2003, pp. 98-429.[§§§§]

[6] Roncoli, R.B., *Lunar Constants and Models Document*, JPL, 2005.[*****]

[††††] For further information on using this service, see http://ssd.jpl.nasa.gov/?horizons (accessed 11 August 2013).

[‡‡‡‡] This document may be downloaded from http://descanso.jpl.nasa.gov/Monograph/series12/LunarTraj--Overall--Compressed.pdf (accessed 25 August 2013).

[§§§§] This document may be downloaded from http://www.boulder.swri.edu/~davidn/papers/irrbig.pdf (accessed 26 August 2013).

[*****] This document may be downloaded from http://ssd.jpl.nasa.gov/dat/lunar_cmd_2005_jpl_d32296.pdf (accessed 11 August 2013).